IEEE Photonics Journal
An IEEE Photonics Society Publication

Design Ultra-Compact Aspherical Lenses for Extended Sources Using Particle Swarm Optical Optimization Algorithm

Volume 11, Number 6, December 2019

Zhengbo Zhu
Shili Wei
Zichao Fan
Yiming Yan
Donglin Ma

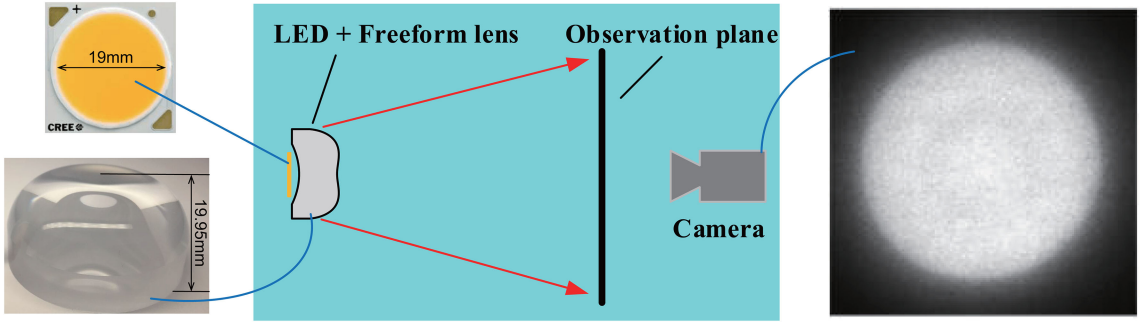

DOI: 10.1109/JPHOT.2019.2951435

Design Ultra-Compact Aspherical Lenses for Extended Sources Using Particle Swarm Optical Optimization Algorithm

Zhengbo Zhu, Shili Wei, Zichao Fan, Yiming Yan, and Donglin Ma

School of Optical and Electronic Information and Wuhan National Laboratory of Opto-Electronics, Huazhong University of Science and Technology, Wuhan 430074, China

DOI:10.1109/JPHOT.2019.2951435

Manuscript received October 6, 2019; revised October 30, 2019; accepted October 31, 2019. Date of publication November 1, 2019; date of current version December 16, 2019. This work was supported in part by the National Natural Science Foundation of China under Grant 61805088, in part by the Fundamental Research Funds for the Central Universities under Grants 2019kfyXKJC040 and 2019kfyRCPY083, and in part by the Wuhan Municipal Science and Technology Bureau under Grant 2019010702011324. Corresponding author: Donglin Ma (e-mail: madonglin@hust.edu.cn).

Abstract: This paper presents a global optimization algorithm specifically tailored for ultra-compact aspherical lens design problems for extended LED sources. The main purpose is to obtain prescribed illumination patterns, particularly the uniform illuminance distribution. This method begins by calculating the initial aspherical lens with two surfaces based on point source approximation. Then a system of polynomials is employed to fit the meridian curves of the two surfaces. In the optimization process, we use the particle swarm optimization (PSO) algorithm to automatically find the optimal polynomial coefficients when the ray tracing simulation is being performed. A series of ultra-compact aspherical lenses with dimension ratio of h/d ranging from 0.95 to 1.25 are presented, where h denotes the center height of the lens and d represents the diameter of the extended source. The results show the high efficiency and versatility of the proposed method in prescribed illumination design for extended LED sources in three-dimensional rotational symmetry geometry. Additionally, an aspherical lens is fabricated and tested, and its practical performance approaches the design.

Index Terms: Extended LED source, prescribed illuminance, illumination design, PSO.

1. Introduction

Realizing accurate control of the spatial energy distribution while maintaining the compactness of the optical system for extended light sources is still a rewarding and urgent task, especially for practical applications such as road lighting illuminations, architectural lighting, etc. [1]–[4]. Since the étendue of an actual light source cannot be neglected in many cases, the design based on point-like source approximation may result in invalid optics designs for actual illumination applications. As a result, to generate exact illumination distributions for extended sources, we need to explore new design methods by taking the source's étendue into consideration.

For zero-étendue cases, the light source is regarded as a point-like source, in which there is only one single ray passing through each point on the optical surfaces [5]. This approximation can lead to an accurate one-to-one ray mapping relationship between source and target [6], [7]. However, this approximation always leads to poor performance in a compact lens design where the dimension ratio of h/d is less than 3 [8]. In these cases, the spatial size or the angular extent of the source

cannot be ignored during the design phase, because there exists a bundle of light rays collected by each point on the optical surfaces [5]. Any facet on the optical surface has a specific normal vector, and thus cannot precisely control all incident light rays under the prescribed regulation.

Up to now, there exist two major categories of freeform optics design methods for extended sources, i.e., the direct design method and the feedback compensation method. The famous simultaneous-multiple-surface (SMS) design method proposed by Benítez, Miñano *et al*. [9] is a powerful tool in illumination design for extended sources. In SMS design method, N freeform surfaces are simultaneously designed to couple N pairs of input/output bundles. The SMS method is a robust and efficient algorithm for extended Lambertian sources, but there still exist difficulties for the direct design method in establishing a specific relationship between the input and output wavefronts. Wu, *et al*. have done many remarkable researches in designing 3D rotational (or freeform) lenses for uniform illumination applications based on the tailored edge-ray principle [5], [10]–[14]. In Ref. [12], a compact aspherical lens with a dimension ratio h/d of 2.53 is demonstrated for a uniform illumination pattern by taking both meridional rays and skew rays of the extended source into account to tailor the lens profiles in the meridional plane. Nevertheless, these methods based on the tailored edge-ray principle are only appropriate for prescribed intensity design where the influence of the lens size on the optical performance can be ignored. Researchers have also proposed traditional feedback compensation methods to deal with the illumination design problems for extended sources [15]–[18], which improve the performance of an optic initially designed with a zero-étendue source through the feedback modification of the lens surfaces based on the simulation result with an actual extended light source. However, these methods are less effective for ultra-compact optical system (for example, $h/d < 2$) designs due to the difficulty in obtaining the global minimum of a specifically defined merit function, such as the relative standard deviation (*RSD*). *RSD* is generally adopted as a performance metric in terms of the uniformity of light distribution.

In this paper, we investigate the optimization technique that aims to find a global optimum solution for rotationally symmetric lens designs with double aspherical surfaces. The method begins by calculating initial surfaces based on a traditional ray mapping algorithm [6], and then the lens profiles are parametrically defined. In the parameter space, the aspherical surfaces are optimized to minimize a predefined merit function. We define the *RSD* of uniformity of the illuminance as the merit function. The global optimization algorithm named particle swarm optimization (PSO) method is employed to drive the global optimization process.

There are three main contributions in this work: (1) the proposed algorithm of global optimization is feasible to design super compact aspherical lenses for prescribed illuminance distribution regardless of whether the lens size can be ignored or not; (2) the double parameterized surfaces of the aspherical lens can be optimized automatically when the simulation is being conducted in the ray tracer. Our proposed design method may provide a new way to design illumination optics for those researchers who are not specialized in mathematics or optics; (3) the proposed method can be applied to design optics with 2D area sources as well as 3D volume sources.

The paper is organized as follows. In Section 2, we give the detailed design principles and procedures of the ultra-compact aspherical lens design problem. In Section 3, several challenge design examples are presented to verify the robustness and efficiency of the proposed method. To validate the workability of the aspherical lens generated by the proposed method, an aspherical lens is fabricated and experimentally measured in Section 4. Finally, a brief conclusion is presented in Section 5.

2. Design Method

The scheme of the proposed design method is illustrated by a flow diagram as shown in Fig. 1. Firstly, we specify the design requirements, such as the source specifications, the target distributions, the lens structure limitations, and so on. Secondly, the surfaces of an initial lens are derived by traditional ray mapping techniques within the point source approximation. After that, we interpolate the initially designed lens surface data into a continuous surface with a polynomial basis. Meanwhile, the merit function is established to evaluate the optical performance for further optimization. Finally,

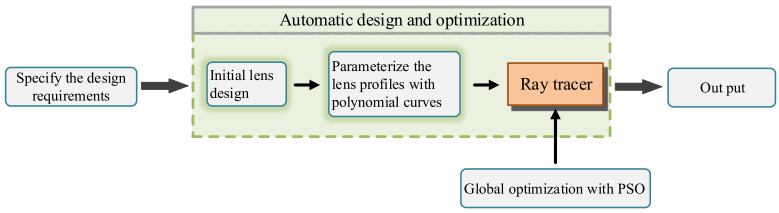

Fig. 1. The design flow chart of the proposed design method.

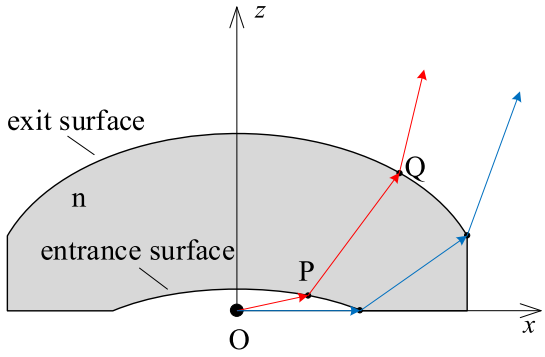

Fig. 2. Designed initial lens model based on the point source approximation.

we modify the coefficients of the polynomials by the heuristic method of PSO algorithms based on the simulation results in the ray tracer. The optimization process stops when the merit function is below the user-defined termination threshold or the number of iterations exceeds the preset value. The whole design process including the initial design and the optimization procedure are carried out automatically.

2.1 Initial Lens Construction and Parameterization

To avoid the total internal reflection (TIR) phenomenon that usually takes place for the LED's secondary optics designed with a plane-aspherical structure, a type of lens with double aspherical surfaces is generally adopted for better light control [14], [19], [20]. The geometrical layout of our designed lens model is shown in Fig. 2. Each ray emitted from the source is firstly refracted by the entrance surface and then redistributed onto the target plane by the exit surface.

In the current design phase, the LED source is considered as a point source and the entire lighting system is axially symmetric. Let us consider designing the aspherical lens generating a prescribed uniform illuminance distribution within a circular region with a radius of R, the lighting distance is $z = H$ and the irradiance value is E_0. The point-like LED source with intensity function $I(\varphi) = I_0 \cos\varphi$, where φ is the viewing angle and I_0 is luminous intensity at the direction of the normal of the source surface, is located at the origin of the Cartesian coordinate system. The entrance surface of the optical element is predefined as a spherical surface shifted in z direction and can be expressed as $C(x, y, z, r_0, z_0) = 0$, where r_0 is the radius of the spherical surface and z_0 is the offset of the sphere's center along z-axis's negative direction. The refractive index of the optical element material is n. With all these specified parameters, we can finally construct the aspherical lens model based on the energy ray mapping mechanism and the geometrical ray propagation principle [21].

Once the initial lens model with double working surfaces is obtained, a system of polynomials is then employed to fit both the entrance surface and the exit surface into two smooth surfaces

respectively as follows:

$$z_p = \sum_{k=1}^{K} \gamma_k \varphi_k \left(x_{ij}, y_{ij}\right), \quad p = 1 \text{ or } 2, \tag{1}$$

where K represents the number of the polynomials, φ_k is the kth polynomial, and γ_k is the weight of φ_k and can be calculated based on the least-square method [22]. For $p = 1$, Eq. (1) represents the inner surface, and specifies the outer surface when $p = 2$. Several types of polynomials and functions can be employed to represent the smooth surfaces including Zernike polynomials, XY polynomials, B-spline functions [23]–[26]. Due to the 3D rotational symmetry of our designed lens model, we only need to characterize the two meridian curves of the entrance surface and the exit surface. As a result, we apply the most simplified XY polynomials to describe the lens profiles because it can provide enough degrees of freedom to guarantee the fitting accuracy.

Therefore, the initial meridian curves of the double aspherical surfaces can be expressed as functions of x and ξ_k $(k = 1, 2, \ldots, K)$ as follows:

$$\begin{cases} z_1 = \sum_{k=1}^{K+1} \xi_{1,k} x_1^{(K+1-k)} \\ z_2 = \sum_{k=1}^{K+1} \xi_{2,k} x_2^{(K+1-k)} \end{cases} \tag{2}$$

where $\xi_{1,k}$ is the kth polynomial coefficient of the inner curve and $\xi_{2,k}$ is the kth polynomial coefficient of the outer curve. It should be emphasized that only the even-term coefficients are retained since the lens profiles are symmetric with respect to the z-axis. Especially noteworthy is that $\xi_{1,K+1}$, and $\xi_{2,K+1}$ denote the central height of the inner surface and the outer surface of the lens respectively, and $\xi_{2,K+1}$ remains unchanged in the subsequent optimization process.

2.2 PSO Algorithm

The PSO algorithm is a population-based stochastic optimization technique developed by Dr. Eberhart and Dr. Kennedy in 1995 [27], [28], inspired by the social behavior of bird flocking or fish schooling. In PSO, there exist a number of individual entities – particles. Each particle represents a potential solution that flies through the search space R^S with velocity by iteratively adjusting flying trajectory (including the direction and magnitude of the velocity) according to its personal experience and its social experience [29]. With each particle evaluating the merit function or objective at each iteration, the swarm as a whole is likely to move close to the optimum of the merit function by using the heuristic rules, which has been widely confirmed in the published literatures [30]–[32]. This character makes it a suitable candidate for global optimization in optical design. The PSO algorithm allows a parallel search, which makes it possible to deal with optimization problems with a large number of variables. Overall, the advantages of PSO algorithm described above make it potentially suitable to be applied to complicated problems such as the aspherical optics design.

The application of the fundamental PSO algorithm to optical design is straightforward. Each certain optical system solution is represented by a particle with a position vector $\boldsymbol{x}_i = (x_{i1}, x_{i2}, \ldots, x_{iS})^T \in R^S$ and a velocity vector $\boldsymbol{v}_i = (v_{i1}, v_{i2}, \ldots, v_{iS})^T \in R^S$ in the S-dimensional search space of variable parameters, in which, S represents the number of variable parameters and i donates the i_{th} iteration. The variable parameters may include thicknesses, refractive indices, or aspherical coefficients. The population size N, i.e., the number of particles, is specified by the designer.

The initial population is generated by adding random of the variable parameters to the optical system that has been obtained above. Once the initial population is specified and the merit function (MF) to evaluate the optical system performance is defined, the PSO algorithm will drive the particles to the most promising optimum. In each iteration, the states of the population will be updated based

on the following rules:

$$\boldsymbol{v}_i^{k+1} = w \cdot \boldsymbol{v}_i^k + c_1 \cdot rand \cdot \left(\boldsymbol{p}_{best}^{ik} - \boldsymbol{x}_i^k\right) + c_2 \cdot rand \cdot \left(\boldsymbol{g}_{best}^{ik} - \boldsymbol{x}_i^k\right) \tag{3}$$

$$\boldsymbol{x}_i^{k+1} = \boldsymbol{x}_i^k + \boldsymbol{v}_i^k \tag{4}$$

where $\boldsymbol{p}_{\text{best}}$ is the personal best position of the particle in history, $\boldsymbol{g}_{\text{best}}$ represents the global best position among all the particles in the current iteration, w is the inertia weight to balance the global and local search abilities, c_1 and c_2 are positive constants named as acceleration coefficients, and rand is a uniformly distributed random number in the interval [0, 1].

The term of c_1 represents a "cognitive "component that pulls a particle back toward its own best position in history, while the "social "component" c_2 drives each particle toward the best position that the swarm has found. Usually, the values of c_1 and c_2 are selected in the range from 0.5 to 2.0 [33]. Large value of w leads to an extensive exploration of the search space, while a small value of w facilitates the local exploration. Relatively better performance will be satisfied if the initially high values of w (typically inside the range of [0.9, 1.2]) gradually decreases during the subsequent iterations [34].

2.3 Optimization Based on PSO Algorithm

Here, *RSD* is employed as the MF to quantify the uniformity of illumination within the target area. Typically, *RSD* is defined as:

$$RSD = \sqrt{\frac{1}{N}\sum_{i=1}^{N_p}\left[\frac{E_s(i) - E_0(i)}{E_0(i)}\right]^2} \tag{5}$$

where N_p is the total number of sampling points inside the effective analysis area on the target surface, $E_s(i)$ is the simulation irradiance level for i_{th} checking point on the target area, and $E_0(i)$ is average of irradiance within the analysis area. A smaller value of *RSD* represents a more uniform illumination performance.

To derive the final lens model for a good illumination performance under the given extended light source, we apply the PSO algorithm to optimize the initial lens structure by minimizing the merit function defined in Eq. (5). The detailed automatic optimization process to design an ultra-compact aspherical lens model based on our proposed PSO algorithm is shown in Fig. 3.

The initial population of N particles is generated by adding small random perturbations to the polynomial coefficients that have been obtained above. The position vector x_i is defined as the corresponding polynomial coefficient ξ_{jk} directly. Considering that small changes of high-order terms can have a great impact on surface profile, we choose the absolute value of velocity vector $\boldsymbol{v}_i$ as $\xi_{jk}/e^{2(K-k+1)}$.

3. Design Examples

3.1 Design Examples for 2D Area Sources

In this section, two types of challenging designs will be given to demonstrate the effectiveness of the proposed method in the prescribed illuminance design for 2D area sources. In the first design, the influence of the lens size on the optical performance can be ignored as the size of the lens is small enough relative to the lighting system. We design an aspherical lens model for a 2D extend source to produce a uniform irradiance distribution onto the target screen. The refractive index of the lens unit is set as 1.4953. The design parameters of the given design examples are listed in Table 1: H denotes the distance between LED source and target, R is the radius of the target plane, h represents the center height of the aspherical lens, d is the diameter of the LED source, and h/d is the dimension ratio of lens model. Besides, the radius r_0 of the incident spherical surface and the offset z_0 of the sphere's center along the z-axis's negative direction in the initial design are 40 mm and 38 mm respectively.

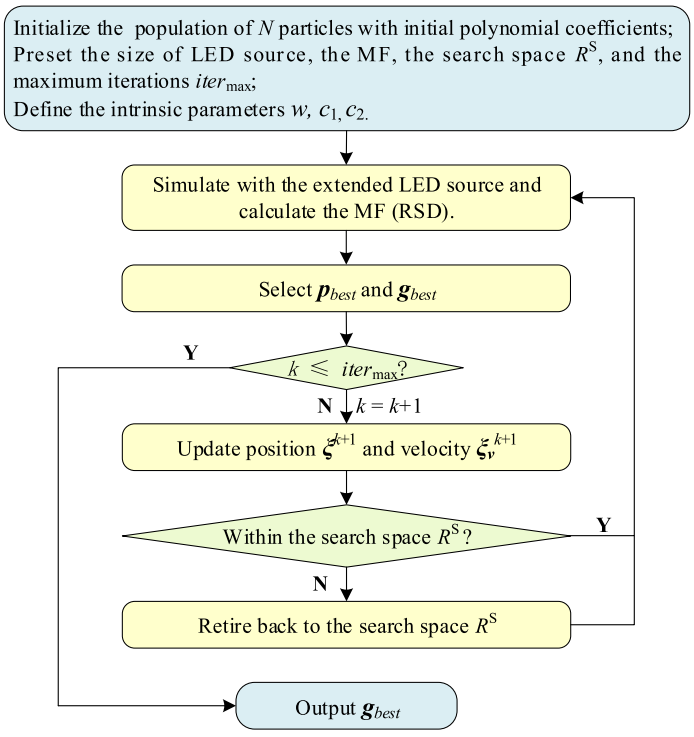

Fig. 3. Flow chart of the PSO algorithm in optimization.

TABLE 1
Design Parameters for the Case Where the Lens Size can be Ignored

H (mm)	R (mm)	h (mm)	d (mm)	h/d
3000	3000	20	16	1.25

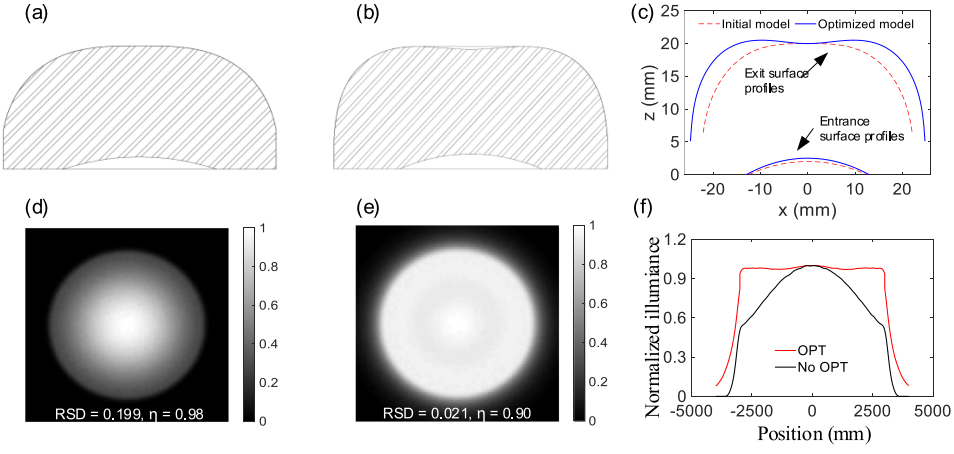

Fig. 4. Design results for the case where the lens size can be ignored: (a) cross-section of the initial lens model; (b) cross-section of the globally optimized lens model; (c) comparison between the cross-section profiles of the two designed lens models; (d) illumination pattern for the initial design; (e) illumination pattern after PSO optimization; (f) comparison between the cross-section profiles of the simulated irradiance patterns for the two designs.

TABLE 2
Design Parameters for the Case Where the Lens Size cannot be Ignored

H (mm)	R (mm)	h (mm)	d (mm)	h/d
100	100	20	16	1.25

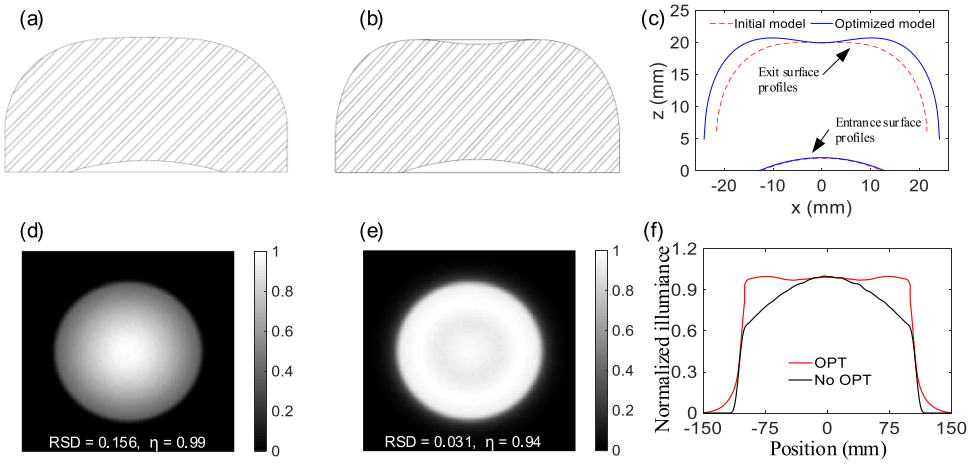

Fig. 5. Design results for the case where the lens size cannot be ignored: (a) cross-section of the initial lens model; (b) cross-section of the globally optimized lens model; (c) comparison between the cross-section profiles of the two designed lens models; (d) illumination pattern for the initial design; (e) illumination pattern after PSO optimization; (f) comparison between the cross-section profiles of the simulated irradiance patterns for the two designs.

Initially, the lenses are designed based on the point source approximation for the specific configurations. Then the curves of the entrance surface and the exit surface are fitted with two series of polynomials up to the 30th order respectively considering both fitting accuracy and time consumption of the optimization process. After that, the PSO algorithm is employed to dynamically adjust the polynomial coefficients based on the predefined MF when the simulation process is being conducted in the ray tracer. The initial population of N is chosen as 40 and the iteration number is set as 20. For all these final obtained lens models, we perform Monte Carlo simulations with 10 million rays to simulate their optical performance.

As a comparison, we also simulate the illumination performance of the initial lens model without the PSO optimization using the same 2D area source as that of the optimized lens model. The simulation results are shown in Fig. 4. The designed lens profiles are illustrated in Fig. 4(a), 4(b) and 4(c). In Fig. 4(f), the red solid line denotes the normalized irradiance profile of the optimized lens model, and the black solid line represents that of the initial lens model without optimization. From Figs. 4(d) and 4(f), we can see that the result of the initial lens without optimization shows a highly concentrated energy distribution in the central portion of the target region. For the optimized lens model, the illumination uniformity is significantly improved as shown in Figs. 4(e) and 4(f). The *RSD* within the target region is reduced from 0.199 to 0.02 while maintaining the energy control efficiency η inside the desired illumination area at a relatively high level. The energy control efficiency η is defined as $\eta = E_{\text{eff}}/E_{\text{total}}$, where E_{eff} is the amount of encircled energy inside the effective analysis area on the target plane, and E_{total} is the amount of total energy on the whole target plane. Obviously, with the help of our proposed global optimization algorithm, we can finally derive an aspherical lens model for extended light sources with a super compact structure compared to the light source, a relatively high illumination uniformity, as well as an acceptable energy control efficiency.

In this second design example, the size of the lens can no longer be ignored relative to the lighting system. The detailed design parameters for the design are listed in Table 2. The simulation

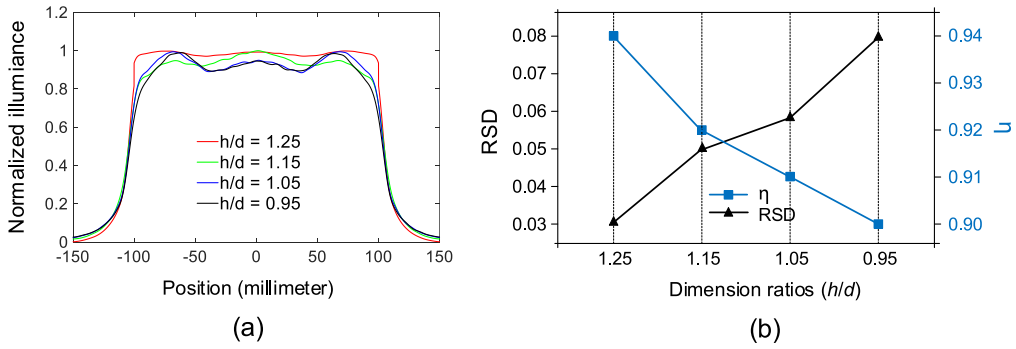

Fig. 6. Simulation results of the optimized lens models with different dimension ratios of h/d, where the lens size cannot be ignored: (a) normalized profiles of illuminance distributions; (b) illuminance uniformity RSD and light energy control efficiency η inside the target region.

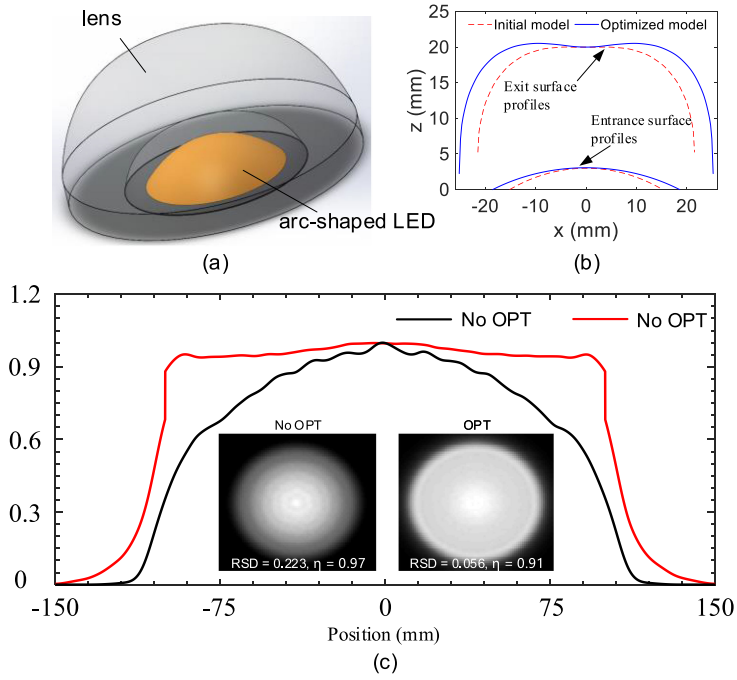

Fig. 7. Design results for 3D volume sources: (a) 3D geometrical layout of the arc-shaped extended source as well as the compact aspherical lens; (b) the lens profiles; (c) comparison of illuminance distributions between the initial lens model and the optimized lens model.

results are demonstrated in Fig. 5. Similarly, a great improvement in illumination uniformity has been achieved after the global optimization algorithm is employed.

To explore the potential of the proposed global optimization algorithm in designing super compact rotationally symmetric lighting applications, we continue to design a series of aspherical lens models with dimension ratios of $h/d = 1.25$, 1.15, 1.05 and 0.95 by gradually increasing the size of LED source (i.e., d) while keeping the center height of lens (i.e., h) and all the other design parameters unchanged. The corresponding simulation results of optimized lens models are shown in Fig. 6. The illuminance uniformity $RSD \leq 0.08$ and light control efficiency $\eta \geq 0.9$ are guaranteed for all dimension ratios of h/d. Even for $h/d = 0.95$, $RSD = 0.08$ and $\eta = 0.9$ could still be obtained.

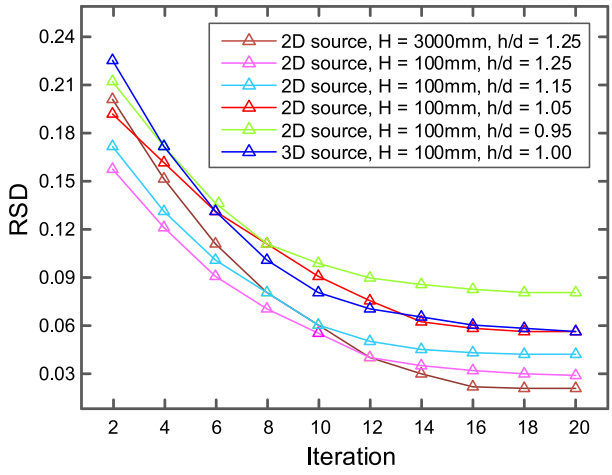

Fig. 8. The convergence of the merit function *RSD*.

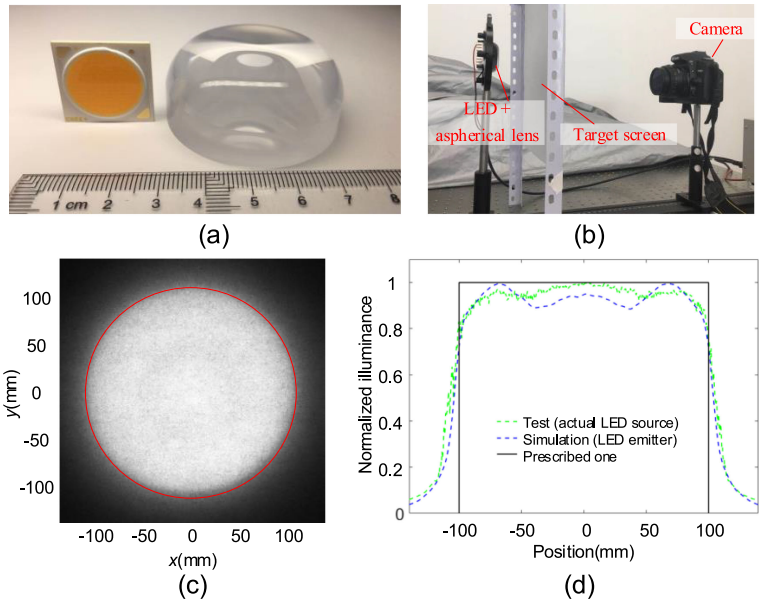

Fig. 9. Experimental verification: (a) the fabricated lens, (b) the experimental setup, (c) the illumination pattern, and (d) the measured illuminance distribution.

3.2 Design Example for 3D Volume Source

Although the proposed method has been successfully applied to illumination designs for the 2D area sources, we still believe that the proposed global optimization algorithm can be generalized to tackle more challenging illumination problems, such as aspherical optics design for 3D volume light sources. To verify the potential of our proposed design algorithm, we design a compact aspherical lens model with the dimension ratio of $h/d = 1.0$ for an arc-shaped extended LED source. The conceptual diagram is schematically shown in Fig. 7(a), where we choose a spherical surface $x^2 + y^2 + (z + 24)^2 = 676(z \geq 0)$ as the emitting surface of the extended light source, and the center height of the entrance surface is chosen as 3.0 mm for the initial design. All the other configurations are set to be the same as that of the Table 2. The simulated illuminance distributions of the initial lens model and the optimized lens model are shown in Fig. 7(c), which demonstrates a significant improvement of optical performance concerning the illuminance uniformity.

TABLE 3
Coefficients of the Polynomials of the Obtained Aspherical Lenses 1 and 2

Coefficients	2D area source, the lens size can be ignored, $H = 3000$, $h = 3000$, $h/d = 1.25$		2D area source, the lens size cannot be ignored, $H = 100$, $h = 20$, $h/d = 1.25$	
	Inner curve	Outer curve	Inner curve	Outer curve
$\xi_{1/2,1}$	1.37020493959549E-46	-2.64713024968586E-37	4.15855802878663E-46	-5.27678137456380E-36
$\xi_{1/2,2}$	0	0	0	0
$\xi_{1/2,3}$	-4.25019065251812E-43	1.05858879099942E-33	-1.20610129906707E-42	2.11771259367916E-32
$\xi_{1/2,4}$	0	0	0	0
$\xi_{1/2,5}$	5.85913642133034E-40	-1.90065166944924E-30	1.57279618101099E-39	-3.81804575600058E-29
$\xi_{1/2,6}$	0	0	0	0
$\xi_{1/2,7}$	-4.79491507582231E-37	2.02213029642968E-27	-1.22247380685311E-36	4.08372549172172E-26
$\xi_{1/2,8}$	0	0	0	0
$\xi_{1/2,9}$	2.55354330631196E-34	-1.41678896402069E-24	6.26191616344790E-34	-2.88238984384211E-23
$\xi_{1/2,10}$	0	0	0	0
$\xi_{1/2,11}$	-9.94050926443003E-32	6.86942106606986E-22	-2.28549345668973E-31	1.41283284957073E-20
$\xi_{1/2,12}$	0	0	0	0
$\xi_{1/2,13}$	1.92396665759077E-29	-2.35557507766516E-19	5.13900414809113E-29	-4.92797090551056E-18
$\xi_{1/2,14}$	0	0	0	0
$\xi_{1/2,15}$	-1.71113075902619E-26	5.72589217709206E-17	-2.28751450066032E-26	1.23269428116733E-15
$\xi_{1/2,16}$	0	0	0	0
$\xi_{1/2,17}$	-2.33300898978422E-23	-9.68630281122437E-15	-2.25904681377420E-23	-2.19909920442304E-13
$\xi_{1/2,18}$	0	0	0	0
$\xi_{1/2,19}$	-4.89612944818802E-20	1.07675820419467E-12	-4.90279231611107E-20	2.74407235415278E-11
$\xi_{1/2,20}$	0	0	0	0
$\xi_{1/2,21}$	-1.04303597823749E-16	-6.38388747514930E-11	-1.04299529656952E-16	-2.30272499926372E-09
$\xi_{1/2,22}$	0	0	0	0
$\xi_{1/2,23}$	-2.38418785270807E-13	-1.19470192361612E-09	-2.38418941406931E-13	1.19490615145806E-07
$\xi_{1/2,24}$	0	0	0	0
$\xi_{1/2,25}$	-6.10306115102307E-10	7.29194551880666E-07	-6.10588456430210E-10	-2.81251829013508E-06
$\xi_{1/2,26}$	0	0	0	0
$\xi_{1/2,27}$	-1.94454922261102E-06	-1.29866279131040E-04	-1.83057376482543E-06	-1.18612606583054E-04
$\xi_{1/2,28}$	0	0	0	0
$\xi_{1/2,29}$	-1.49207592274027E-02	1.34044883544090E-02	-1.19921452956317E-02	1.81426009315680E-02
$\xi_{1/2,30}$	0	0	0	0
$\xi_{1/2,31}$	2.45298594027405E+00	20	1.93012945309807E+00	20

The convergences of the merit function *RSD* of the above designs are shown in Fig. 8. The values of *RSD* reach steady states after 20 times of iteration steps. And the running time of the optimizations of these designs is no more than 10 minutes on Intel Xeon E3-1230 v3 with 16 GB RAM. All the polynomial coefficients of the final obtained lens models above are tabulated in the Appendix.

4. Experiment

To verify the feasibility of our proposed design algorithms, we fabricate a prototype by using the Single Point Diamond Turning Techniques. This lens is chosen with the dimension ratio $h/d = 1.05$ which is designed above, where the lighting distance $H = 100$ mm, as shown in Fig. 9(a). We choose Cree's chip-on-board (COB) LEDs CXB2540 [35] as the light source. The diameter of the effective emitting area of the LED emitter is 19.00 mm. The lens material is PMMA, whose refractive index is about 1.49. To avoid the blockage, we place the camera in front of the target plane to record the light distribution. The experimental setup is as shown in Fig. 9(b). The captured pattern and the

TABLE 4
Coefficients of the Polynomials of the Obtained Aspherical Lenses 3 and 4

Coefficients	2D area source, the lens size cannot be ignored, $H = 100$, $h = 20$, $h/d = 1.15$		2D area source, the lens size cannot be ignored, $H = 100$, $h = 20$, $h/d = 1.05$	
	Inner curve	Outer curve	Inner curve	Outer curve
$\xi_{1/2,\,1}$	4.15855802878663E-46	-2.29445615073726E-36	4.15855802878663E-46	-1.23374899193559E-36
$\xi_{1/2,\,2}$	0	0	0	0
$\xi_{1/2,\,3}$	-1.20610129906707E-42	9.53586796956169E-33	-1.20610129906707E-42	5.25893867703115E-33
$\xi_{1/2,\,4}$	0	0	0	0
$\xi_{1/2,\,5}$	1.57279618101099E-39	-1.78009481410104E-29	1.57279618101099E-39	-1.00665107773197E-29
$\xi_{1/2,\,6}$	0	0	0	0
$\xi_{1/2,\,7}$	-1.22247380685311E-36	1.97088337202647E-26	-1.22247380685311E-36	1.14251790391161E-26
$\xi_{1/2,\,8}$	0	0	0	0
$\xi_{1/2,\,9}$	6.26191616344790E-34	-1.43947920709603E-23	6.26191616344790E-34	-8.55035940792824E-24
$\xi_{1/2,\,10}$	0	0	0	0
$\xi_{1/2,\,11}$	-2.28549345668973E-31	7.29731853098895E-21	-2.28549345668973E-31	4.43852291424705E-21
$\xi_{1/2,\,12}$	0	0	0	0
$\xi_{1/2,\,13}$	5.13900414809113E-29	-2.63031369851294E-18	5.13900414809113E-29	-1.63660269021970E-18
$\xi_{1/2,\,14}$	0	0	0	0
$\xi_{1/2,\,15}$	-2.28751450066032E-26	6.79019036254514E-16	-2.28751450066032E-26	4.31475754803331E-16
$\xi_{1/2,\,16}$	0	0	0	0
$\xi_{1/2,\,17}$	-2.25904681377430E-23	-1.24715094948023E-13	-2.25904681377422E-23	-8.06900618395709E-14
$\xi_{1/2,\,18}$	0	0	0	0
$\xi_{1/2,\,19}$	-4.90279231611730E-20	1.59440810023031E-11	-4.90279231610163E-20	1.04374353851278E-11
$\xi_{1/2,\,20}$	0	0	0	0
$\xi_{1/2,\,21}$	-1.04299529648844E-16	-1.35433939673179E-09	-1.04299529680578E-16	-8.82564028257984E-10
$\xi_{1/2,\,22}$	0	0	0	0
$\xi_{1/2,\,23}$	-2.38418941059366E-13	6.81914070706294E-08	-2.38418943925672E-13	4.14973051418589E-08
$\xi_{1/2,\,24}$	0	0	0	0
$\xi_{1/2,\,25}$	-6.11107822793676E-10	-1.06122661398846E-06	-6.10312193192620E-10	-8.85129294790995E-08
$\xi_{1/2,\,26}$	0	0	0	0
$\xi_{1/2,\,27}$	-1.95480912591754E-06	-1.59367422151254E-04	-1.94067309327111E-06	-1.89728829069346E-04
$\xi_{1/2,\,28}$	0	0	0	0
$\xi_{1/2,\,29}$	-1.27359491229261E-02	2.06910526511611E-02	-1.25206394216159E-02	2.46446673899386E-02
$\xi_{1/2,\,30}$	0	0	0	0
$\xi_{1/2,\,31}$	1.99324194512665E+00	20	1.98352075126406E+00	20

measured illumination distribution along with the line $y = 0$ mm are depicted in Figs. 9(c) and 9(d). The experimental testing results demonstrate relatively high agreement with our simulation results, which proves that our proposed design optimization algorithm is highly efficient for the design of ultra-compact aspherical lenses based on extended sources. The fabrication errors and alignment errors are the two main error sources that contribute to minor differences. The *RSD* and energy control efficiency η are equal to 0.073 and 0.89 respectively within the prescribed region with a radius of 100.00 mm.

5. Conclusion

In the paper, we develop a global optimization algorithm to design ultra-compact aspherical lenses to transfer the light emitted from extended light sources to uniform illumination distributions on the target plane. The design algorithm is based on the heuristic rules of PSO and can be conducted automatically by non-experts in optics design. Many illumination design examples for extended sources are developed to verify the efficiency of the proposed design method. Simulation results

TABLE 5
Coefficients of the Polynomials of the Obtained Aspherical Lenses 5 and 6

Coefficients	2D area source, the lens size cannot be ignored, $H = 100$, $h = 20$, $h/d = 0.95$		3D volume source, the lens size cannot be ignored, $H = 100$, $h = 20$, $h/d = 1.00$	
	Inner curve	Outer curve	Inner curve	Outer curve
$\xi_{1/2,\,1}$	4.1585580287866E-46	-6.6484692661438E-37	7.42370537411381E-48	-1.0455904755280E-35
$\xi_{1/2,\,2}$	0	0	0	0
$\xi_{1/2,\,3}$	-1.20610129906707E-42	2.90369061107457E-33	-2.89750550201117E-44	4.66671065963591E-32
$\xi_{1/2,\,4}$	0	0	0	0
$\xi_{1/2,\,5}$	1.57279618101099E-39	-5.69301344790167E-30	4.60547264942522E-41	-9.35642172914701E-29
$\xi_{1/2,\,6}$	0	0	0	0
$\xi_{1/2,\,7}$	-1.22247380685311E-36	6.61502450489384E-27	-4.51286196990004E-38	1.11291142373214E-25
$\xi_{1/2,\,8}$	0	0	0	0
$\xi_{1/2,\,9}$	6.26191616344790E-34	-5.06480161862377E-24	2.54122816106996E-35	-8.73681995635160E-23
$\xi_{1/2,\,10}$	0	0	0	0
$\xi_{1/2,\,11}$	-2.28549345668973E-31	2.68711653565569E-21	-1.49176505669309E-32	4.76459806959113E-20
$\xi_{1/2,\,12}$	0	0	0	0
$\xi_{1/2,\,13}$	5.13900414809113E-29	-1.01105199092480E-18	-2.90508905676588E-30	-1.85014295434185E-17
$\xi_{1/2,\,14}$	0	0	0	0
$\xi_{1/2,\,15}$	-2.28751450066032E-26	2.71277940484201E-16	-1.29224200266542E-26	5.15819019120972E-15
$\xi_{1/2,\,16}$	0	0	0	0
$\xi_{1/2,\,17}$	-2.25904681377422E-23	-5.13765431462029E-14	-2.39016780638833E-23	-1.02796566562213E-12
$\xi_{1/2,\,18}$	0	0	0	0
$\xi_{1/2,\,19}$	-4.90279231610109E-20	6.65902992726030E-12	-4.89057192589655E-20	1.43995320703741E-10
$\xi_{1/2,\,20}$	0	0	0	0
$\xi_{1/2,\,21}$	-1.04299529681365E-16	-5.47837766552443E-10	-1.04307345068145E-16	-1.37343560116447E-08
$\xi_{1/2,\,22}$	0	0	0	0
$\xi_{1/2,\,23}$	-2.38418942007050E-13	2.17484206275801E-08	-2.38418610686633E-13	8.44629322215768E-07
$\xi_{1/2,\,24}$	0	0	0	0
$\xi_{1/2,\,25}$	-6.10341908706967E-10	6.79882468592113E-07	-6.10023552562270E-10	-3.01821983114137E-05
$\xi_{1/2,\,26}$	0	0	0	0
$\xi_{1/2,\,27}$	-1.96858600391001E-06	-2.12734835499155E-04	-2.04873376167712E-06	4.20127093469999E-04
$\xi_{1/2,\,28}$	0	0	0	0
$\xi_{1/2,\,29}$	-1.22397089930636E-02	2.67519335933089E-02	-8.55070350952455E-03	1.10694486303724E-02
$\xi_{1/2,\,30}$	0	0	0	0
$\xi_{1/2,\,31}$	1.99126791467182E+00	20	3.39112594539240E+00	20

show that the design method can realize the desired illumination patterns even for a super compact lens model with dimension ratio h/d less than 1.0. Besides, the proposed design algorithm can be applied to design optics in generating prescribed illumination patterns for both 2D area sources and 3D volume sources. We also demonstrate the effectiveness of our proposed method by prototyping one of the designed lenses, where the experimental performance is quite consistent with our simulation result.

In future work, we will apply the global optimization technique to tackle more challenging illumination design problems for extended light sources, such as non-rotationally symmetric lighting systems.

Appendix
Coefficients of the Polynomials

As expressed in Eq. (2), where ξ_1, k is the kth polynomial coefficient of the inner curve and ξ_2, k is the kth polynomial coefficient of the outer curve. All these coefficients are detailed in the following Table 3, Table 4 and Table 5.

Acknowledgment

The authors would like to thank the anonymous reviewers for their valuable suggestions.

References

[1] C. C. Sun *et al.*, "Design of LED street lighting adapted for free-form roads," *IEEE Photon. J.*, vol. 9, no. 1, Feb. 2017, Art. no. 8200213.
[2] X. Sun, L. Kong, and M. Xu, "Uniform illumination for nonplanar surface based on freeform surfaces," *IEEE Photon. J.* vol. 11, no. 3, Jun. 2019, Art. no. 2200511.
[3] C. M. Tsai, and B. X. Wang, "A freeform mirror design of uniform illumination in streetlight from a split light source," *IEEE Photon. J.* vol. 10, no. 4, Aug. 2018, Art. no. 2201212.
[4] R. Zhu, Q. Hong, H. Zhang, and S. T. Wu, "Freeform reflectors for architectural lighting," *Opt. Exp.*, vol. 23, no 25, pp. 31828–31837, 2015.
[5] R. Wu and H. Hua, "Direct design of aspherical lenses for extended non-Lambertian sources in three-dimensional rotational geometry," *Opt. Exp.*, vol. 24, no. 2, pp. 1017–1030, 2016.
[6] Z. Zheng, H. Xiang, and L. Xu, "Freeform surface lens for LED uniform illumination," *Appl. Opt.*, vol. 48, no. 35, pp. 6627–6634, 2009.
[7] Y. Luo, Z. Feng, Y. Han, and H. Li, "Design of compact and smooth free-form optical system with uniform illuminance for LED source," *Opt. Exp.*, vol. 18, no. 9, pp. 9055–9063, 2010.
[8] K. Wang, Y. Han, H. Li, and Y. Luo, "Overlapping-based optical freeform surface construction for extended lighting source," *Opt. Exp.*, vol. 21, no. 17, pp. 19750–19761, 2013.
[9] P. Gimenez-Benitez *et al.*, "Simultaneous multiple surface optical design method in three dimensions," *Opt. Eng.*, vol. 43, no. 7, pp. 1489–1503, 2004.
[10] X. Mao, H. Li, Y. Han, and Y. Luo, "A two-step design method for high compact rotationally symmetric optical system for LED surface light source," *Opt. Exp.*, vol. 22, no. S2, pp. A233–A247, 2014.
[11] R. Wu, H. Hua, P. Benítez, and J. C. Miñano, "Direct design of aspherical lenses for extended non-Lambertian sources in two-dimensional geometry," *Opt. Lett.*, vol. 40, no. 13, pp. 3037–3040, 2015.
[12] R. Wu, C. Y. Huang, X. Zhu, H.-N. Cheng, and R. Liang, "Direct three-dimensional design of compact and ultra-efficient freeform lenses for extended light sources," *Optica*, vol. 3, no. 8, pp. 840–843, 2016.
[13] X. Li, P. Ge, and H. Wang, "Prescribed intensity in 3D rotational geometry for extended sources by using a conversion function in 2D design," *Appl. Opt.*, vol. 56, no. 6, pp. 1795–1798, 2017.
[14] S. Hu, K. Du, T. Mei, L. Wan, and N. Zhu, "Ultra-compact LED lens with double freeform surfaces for uniform illumination," *Opt. Exp.*, vol. 23, no. 16, pp. 20350–20355, 2015.
[15] Y. Luo, Z. Feng, Y. Han, and H. Li, "Design of compact and smooth free-form optical system with uniform illuminance for LED source," *Opt. Exp.*, vol. 18, no. 9, pp. 9055–9063, 2010.
[16] K. Wang, Y. Han, H. Li, and Y. Luo, "Overlapping-based optical freeform surface construction for extended lighting source," *Opt. Exp.*, vol. 21, no. 17, pp. 19750–19761, 2013.
[17] R. Wester, G. Müller, A. Völl, M. Berens, J. Stollenwerk, and P. Loosen, "Designing optical free-form surfaces for extended sources," *Opt. Exp.*, vol. 22, no. S2, pp. A552–A560, 2014.
[18] Z. Zhu, Y. Yan, S. Wei, Z. Fan, and D. Ma, "Compact freeform primary lens design based on extended Lambertian sources for liquid crystal display direct-backlight applications," *Opt. Eng.*, vol. 58, no. 3, pp. 025108-1–025108-8, 2019.
[19] M. A. Moiseev, S. V. Kravchenko, and L. L. Doskolovich, "Design of efficient LED optics with two free-form surfaces," *Opt. Exp.*, vol. 22, no. S7, pp. A1926–A1935, 2014.
[20] H. Wu, X. Zhang, and P. Ge, "Double freeform surfaces lens design for LED uniform illumination with high distance–height ratio," *Opt. Laser Technol.*, vol. 73, pp. 166–172, 2015.
[21] Z. Zheng, H. Xiang, and L. Xu. "Freeform surface lens for LED uniform illumination," *Appl. Opt.*, vol. 48, no. 35, pp. 6627–6634, 2019.
[22] J. Zhu, X. Wu, T. Yang, and G. Jin, "Generating optical freeform surfaces considering both coordinates and normals of discrete data points," *J. Opt. Soc. Amer.*, vol. 31, no. 11, pp. 2401–2408, 2014.
[23] R. Wu, J. Sasián, and R. Liang, "Algorithm for designing free-form imaging optics with nonrational b-spline surfaces," *Appl. Opt.*, vol. 56, no. 9, pp. 2517–2522, 2017.
[24] M. Moiseev and L. Doskolovich, "Design of refractive spline surface for generating required irradiance distribution with large angular dimension," *J. Modern Opt.*, vol. 57, no. 7, pp. 536–544, 2010.
[25] G. W. Forbes, "Characterizing the shape of freeform optics," *Opt. Exp.*, vol. 20, no. 3, pp. 2483–2499, 2012.
[26] X. Mao, J. Li, F. Wang, R. Gao, X. Li, and Y. Xie, "Fast design method of smooth freeform lens with an arbitrary aperture for collimated beam shaping," *Appl. Opt.*, vol. 58, no. 10, pp. 2512–2521, 2019.
[27] J. Kennedy and R. Eberhart, "Particle swarm optimization," in *Proc. IEEE Conf. Neural Netw.*, 1995, vol. 4, pp. 1942–1948.

[28] R. Eberhart and J. Kennedy, "A new optimizer using particle swarm theory," in *Proc. Micro Mach. Hum. Sci.*, 1995, pp. 39–43.
[29] N. D. Jana, J. Sil, and S. Das, "Particle swarm optimization with population adaptation," in *Proc. IEEE Congr. Evol. Comput.,* 2014, pp. 573–578.
[30] M. R. Bonyadi and Z. Michalewicz, "Particle swarm optimization for single objective continuous space problems: A review," *Evol. Comput.*, vol. 25, no. 1, pp. 1–54, 2017.
[31] Z. Fan, S. Wei, Z. Zhu, Y. Mo, Y. Yan, and D. Ma, "Automatically retrieving an initial design of a double-sided telecentric zoom lens based on a particle swarm optimization," *Appl. Opt.*, vol. 58, no. 27, pp. 7379–7386, 2019.
[32] K. E. Parsopoulos and M. N. Vrahatis, "Recent approaches to global optimization problems through particle swarm optimization," *Natural Comput.*, vol. 1, no. 2/3, pp. 235–306, 2002.
[33] C. Menke, "Application of particle swarm optimization to the automatic design of optical systems," *Proc. SPIE*, vol. 10690, 2018, Art. no. 106901A.
[34] R. Eberhart and J. Kennedy, "A new optimizer using particle swarm theory," in *Proc. Micro Mach. Hum. Sci.*, 2002, pp. 39–43.
[35] [Online]. Available: https://www.cree.com/led-components/products/xlamp-leds-integrated-arrays/xlamp-cxb2540